Research article **Open Access**

Teng-Fei Zhang, Guo-An Wu, Jiu-Zhen Wang, Yong-Qiang Yu, Deng-Yue Zhang, Dan-Dan Wang, Jing-Bo Jiang, Jia-Mu Wang and Lin-Bao Luo*

A sensitive ultraviolet light photodiode based on graphene-on-zinc oxide Schottky junction

DOI 10.1515/nanoph-2016-0143
Received August 11, 2016; revised September 27, 2016; accepted October 11, 2016

Abstract: In this study, we present a simple ultraviolet (UV) light photodiode by transferring a layer of graphene film on single-crystal ZnO substrate. The as-fabricated heterojunction exhibited typical rectifying behavior, with a Schottky barrier height of 0.623 eV. Further optoelectronic characterization revealed that the graphene-ZnO Schottky junction photodiode displayed obvious sensitivity to 365-nm light illumination with good reproducibility. The responsivity and photoconductive gain were estimated to be 3×10^4 A/W and 10^5, respectively, which were much higher than other ZnO nanostructure-based devices. In addition, it was found that the on/off ratio of the present device can be considerably improved from 2.09 to 12.1, when the device was passivated by a layer of AlO_x film. These results suggest that the present simply structured graphene-ZnO UV photodiode may find potential application in future optoelectronic devices.

Keywords: graphene; Schottky junction; UV photodetector; responsivity; surface passivation.

1 Introduction

Zinc oxide (ZnO), with a wide direct band gap (3.4 eV) and a large exciton binding energy of 60 meV, has been one of the most studied II–VI group semiconductors [1]. In comparison to their bulk and thin film counterparts, ZnO nanostructures in one-dimensional (1D) form including nanowires [2], nanoribbons [3], and nanorods [4, 5] have exhibited excellent electrical and optical properties due to the quantum size effect and large surface-to-volume ratio [4, 6]. For this reason, 1D ZnO nanostructures have been widely employed to fabricate various electronic and opto-electronic devices including chemical and biological sensors [7, 8], field effect transistors (FETs) [9, 10], photovoltaic devices [11, 12], light-emitting diodes (LEDs) [13, 14], lasers[15, 16], and photodetectors [17, 18]. Among these nanodevices, photodetectors based on ZnO nanostructures have recently received increasing research interest due to their wide application in various military fields including emitter calibration, spatial optical communication, and light vision and so on [19]. For instance, Soci et al. developed a high-performance visible-blind photodetector based on individual ZnO nanowire (ZnONW) [20]. They found that the internal photoconductive gain was as high as 10^8, the highest value ever reported. More recently, we reported a graphene-ZnO nanorod (ZnONR) array Schottky junction UV photodetector. Thanks to the novel device geometry, the graphene-ZnO device exhibited a high responsivity of 113 A/W, and a fast response rate of millisecond [21].

In spite of these progresses, it is undeniable that most of the ZnO nanostructure photodetectors are characterized by the following two features: (1) Relatively complicated fabrication process. The device assembly normally involves the synthesis of ZnO nanostructures, which is difficult to precisely control the diameter and surface states of the final product. (2) Poor device reliability. Owing to the lack of precise control over individual nanostructures, the device performance is often different from one another, leading to poor device reproducibility and reliability. Without question, these problems have constituted the main bottleneck for their practical application. In light of this, we herein report a simple and sensitive UV light photodetector by directly transferring a layer of chemical vapor deposition (CVD) graphene on a commercial single-crystal ZnO wafer. It was found that the as-fabricated graphene-ZnO heterojunction exhibited typical rectifying characteristics with a Schottky barrier height of 0.623 eV.

***Corresponding author: Lin-Bao Luo,** School of Microelectronics, Hefei University of Technology, Hefei, Anhui 230009, P. R. China, e-mail: luolb@hfut.edu.cn
Teng-Fei Zhang, Guo-An Wu, Jiu-Zhen Wang, Yong-Qiang Yu, Deng-Yue Zhang, Dan-Dan Wang, Jing-Bo Jiang and Jia-Mu Wang: School of Microelectronics, Hefei University of Technology, Hefei, Anhui 230009, P. R. China

What is more, the graphene-ZnO Schottky junction photodiode was highly sensitive to a 365-nm light illumination with good reproducibility. The responsivity, photoconductive gain, and detectivity were estimated to be 3×10^4 A/W, 10^5, and 4.33×10^{14} Jones, respectively, which are much better than other photodetectors based on ZnO nanostructures. It was also revealed that when the device was passivated by a layer of AlO_x film, the on/off ratio of the present device can be considerably improved from 2.09 to 12.01. The above results suggest that the present simply structured graphene-ZnO UVPD is a promising building block for fabricating high-performance optoelectronic devices.

2 Results and discussion

Figure1A shows a typical schematic illustration of the graphene-ZnO Schottky UVPD. To fabricate the device, commercial ZnO wafers were first cleaned in acetone, alcohol, and deionized water, respectively. Afterwards, 5-nm Ti and 50-nm Au were deposited on the ZnO back surface to form *Ohmic* contact. Graphene synthesized via CVD method was then transferred onto the surface of clean *n*-type ZnO substrate, leading to the formation of Schottky junction with a junction area of 4×2.5 mm^2 (Figure 1B). Figure 1C shows the Raman spectrum of the graphene film, from which one can observe two obvious peaks, i.e. a 2D band peak at ~2680 cm^{-1} and a *G* band peak at ~1590 cm^{-1}. The intensity ratio of $I_{2D}:I_G$ is estimated to be 2:1, signifying the single layer of the graphene. What is more, the weak D-band scattering at ~1340 cm^{-1} indicates the low-density defects of the graphene film [22, 23]. This graphene-ZnO Schottky junction can function as an efficient UVPD, whose operation mechanism can be understood from the energy band diagram illustrated in Figure 1D. The work function of graphene and ZnO are 4.6 and 4.4 eV, respectively. When graphene and ZnO are in contact to each other, the energy band bends upward as the surface of the energy of a semiconductor is higher than the body. As a result, the ZnO surface will form a space charge region (built-in electric field) with a direction pointing from the body to the surface. At reverse bias voltage, the energy band of ZnO continues to bend upward, leading to a strengthened barrier height at the interface. Thus, it is difficult for the electrons to enter through the space charge region from ZnO to graphene, which corresponds to an "off" state characterized by low dark current. When irradiated with UV light with sufficient energy, the electrons of the valence band are excited into the conduction band, and holes are generated in the valence band. The

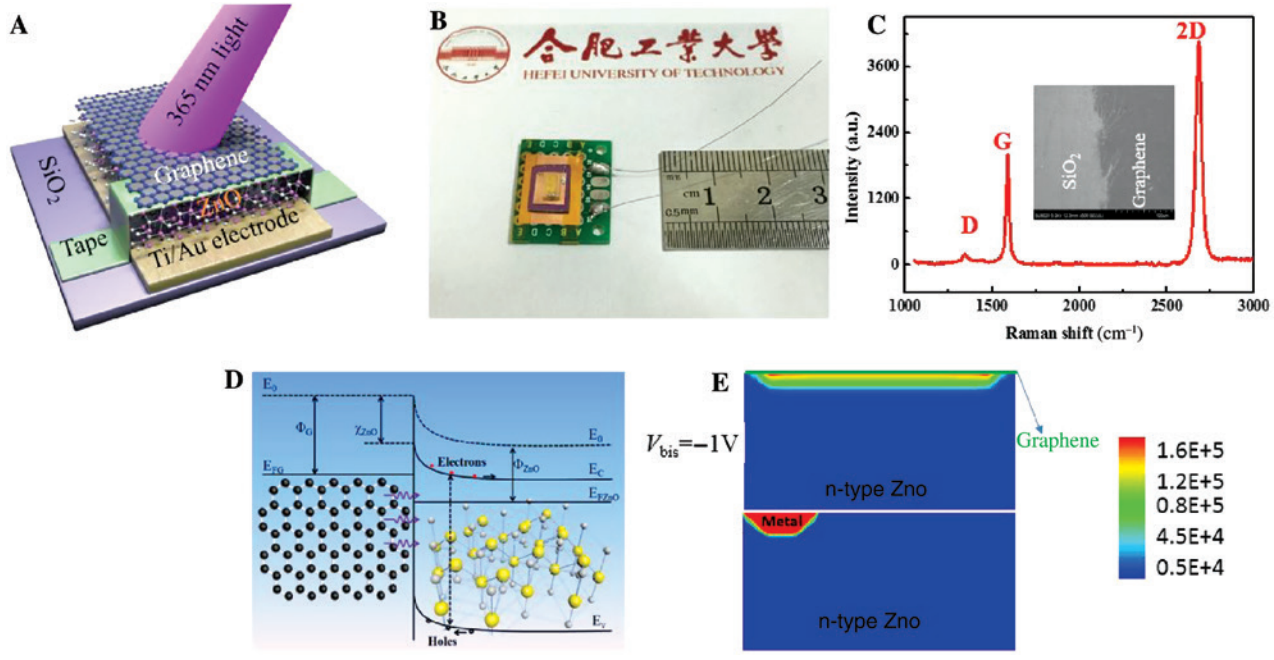

Figure 1: (A) Schematic illustration of the graphene-ZnO Schottky junction photodiode. (B) A representative digital camera picture of the UVPD device. (C) Raman spectrum of the graphene film; the inset shows an SEM image of the graphene film on a SiO_2-Si substrate. (D) Energy band diagram of the UVPD under UV light illumination at a reverse bias. (E) The total current density distribution of graphene-ZnO and metal-ZnO device at a bias voltage of – 1 V.

photo-generated electron-hole pairs in the space-charge region are separated by the built-in field, constituting the photocurrent in external circuit. It should be pointed out that the present graphene-ZnO Schottky junction is good at collecting carriers for the complete coating of graphene. Figure 1E compares the total current density distribution of both graphene-ZnO and metal-ZnO structure at a bias voltage of −1 V, which was carried out by a 2D semiconductor simulation package (ISE-TCAD). We can see that the 100% coverage of transparent and metallic graphene on the ZnO surface will lead to homogenous current distribution all over the graphene-ZnO contact. On the contrary, the metal-ZnO device, which is characterized by partial coating of metal on the ZnO surface [24], has a relatively inhomogeneous current distribution. Undoubtedly, this superb electrical characteristic is greatly beneficial for the carrier collection, which is of paramount importance to efficient UV light detection.

Thanks to the metallic property of the graphene film, the present graphene-ZnO heterojunction exhibits a typical rectifying behavior with a turn-on voltage of 0.18 V, as shown in Figure 2A. Such a rectifying characteristic arises from the Schottky barrier of the graphene-ZnO contact, which can be described by the thermionic emission-based diode equation [25]:

$$J(T,V) = J_s(T)\left[\exp\left(\frac{eV}{\eta K_B T}\right) - 1\right] \quad (1)$$

where $J(T, V)$ is the current density across the graphene film-ZnO interface, V is the applied voltage, k_B is the Boltzmann's constant, T is the absolute temperature, and n is the ideality factor [$n = (q/kT)(dV/d\ ln\ I)$]. The prefactor, $J_s(T)$ is the saturation current density and can be described by $J_s(T) = A{*}T^2\exp(-e\phi_{SBH}/K_B T)$, where ϕ_{SBH} is the zero bias Schottky barrier height (SBH), $A{*}$ is the Richardson constant, and $m{*}$ is the effective mass of the charge carriers, respectively. For ZnO material, $A{*}$ is theoretically calculated to be 32 A cm^{-2} k^{-2} ($m_e^* = 0.27m_0$); using the J_s value, the Schottky barrier height at the graphene-ZnO interface is estimated to be 0.623 eV, which is comparable to that of graphene-ZnONR array [20] and graphene-TiO_2 nanotube array [26]. When shined by UV light with a wavelength of 365 nm, the graphene-ZnO Schottky junction photodiode displays obvious photosensitivity. Figure 2B shows a family of *I-V* curves obtained in the range from light intensity (from 0.9 to 493 μW/cm^2). The photocurrent will increase gradually with increasing light intensity at negative bias voltage. However, it is interesting to note that the SLG-ZnO detector is virtually blind to UV light in the forward bias voltage. For such graphene-ZnO Schottky junction devices, due to the metallic behavior as well the excellent optical property, the graphene actually act as a transparent electrode, which plays two important roles: First, like conventional metal, the graphene can form a good Schottky junction with the single-crystal ZnO wafer, which is capable of separating the photo-excited carriers by the built-in electric field. Second, as the absorption of single-layer graphene is only 2.3%, the majority of the incident light can penetrate the graphene layer and reach the underlying ZnO wafer. In other words, the graphene actually functions as a transparent electrode. Further photoresponse study reveals that, although the present device is quite sensitive to variation of UV light intensity (Figure 2C), the relationship between both photocurrent and light intensity cannot be described by the well-accepted power law formula that has been widely used in a previous study [27]. Figure 2D shows the photocurrent as a function of light intensity, from which we can learn that in the low range from 0 to 320 μW/cm^2, the photocurrent will gradually increase with increasing intensity, but with further increase in the intensity, the photocurrent, on the contrary, begins to saturate. Figure 2E plots the switchable photoresponse of the graphene-ZnO device when the 365-nm irradiation was switched on and off repeatedly. It is obvious that the UVPD can be reversibly switched between "on" and "off" states with excellent reproducibility. By deducing the response curve, the rise and fall time were estimated to be <1 s and 22 s, respectively. Such relatively slow response rate is probably due to the existence of defects species (e.g. O or Zn vacancies, and the excess of Zn and O atoms) that can act as efficient recombination centers to trap the carriers and, therefore, extend the time of the recombination [28]. Remarkably, the present device is highly stable even though it was stored in ambient condition for long term. Figure 2E shows the photoresponse of the same device after storage for 3 months. The photocurrent was virtually identical to the fresh one without obvious decay, which suggests excellent device stability.

It was interesting to note that the photosensitivity of graphene-ZnO is dependent on the bias voltage. Figure 3A displays the photoresponse of the device at various bias voltages. It can be seen that with the gradual increase in the bias voltage from −2 to −5 V, both dark current and photocurrent are observed to increase accordingly. From the numerical relationship between the on-off ratio and bias voltage (Figure 3B), one can learn that in low bias voltage range from −1 to −6 V, the on-off ratio increases with the increasing bias voltage. However, with the further decrease in the bias voltage, the on-off ratio begins to decrease. In order to quantitatively assess the device performance of the UVPD, two

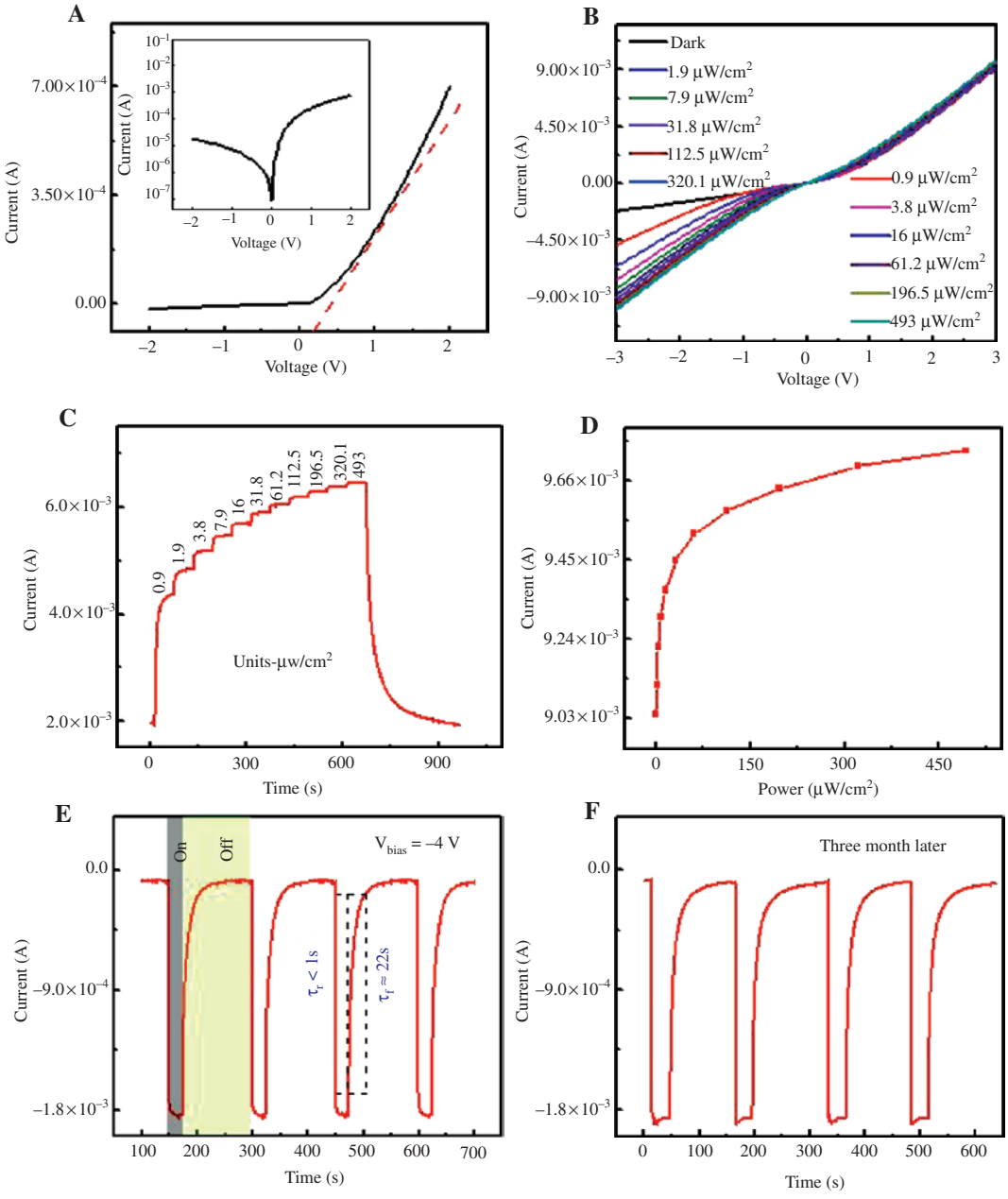

Figure 2: (A) *I-V* curves of the graphene-ZnO Schottky diode; the inset shows the *I-V* curve at a log scale. (B) *I-V* characteristics of the graphene-ZnO UVPD under 365-nm light illumination with various power intensities. (C) Time response of the UVPD under 365 nm with various power intensities. (D) The relationship between the photocurrent and intensity. (E) Photoresponse of the graphene-ZnO UVPD under 365-nm light illumination. (F) Photoresponse of the UVPD after storage for 3 months.

key device parameters including both responsivity (R) and photoconductive gain (G) were calculated by the following formulas [29]:

$$R = \frac{I_p - I_d}{P_{opt}} = \frac{\Delta I}{P_{opt}} = \eta\left(\frac{q\lambda}{hc}\right)G \quad (2)$$

$$G = R\frac{hc}{\eta q\lambda} \quad (3)$$

where I_p, I_d, P_{opt}, η, q, λ, h, and c are the photocurrent, the current without light illuminated on, the power of the light that is irradiated on the device, the quantum efficiency (assuming $\eta = 1$ for convenience) [18], the absolute value of electron charge (1.6×10^{-19} Coulombs), the wavelength of illuminated light (365 nm), the Planck's constant (6.626×10^{-34} J·s), and the velocity of light (3×10^8 m/s), respectively. Based on the above constants and Equations 2 and 3, the responsivity and photoconductive gain at a

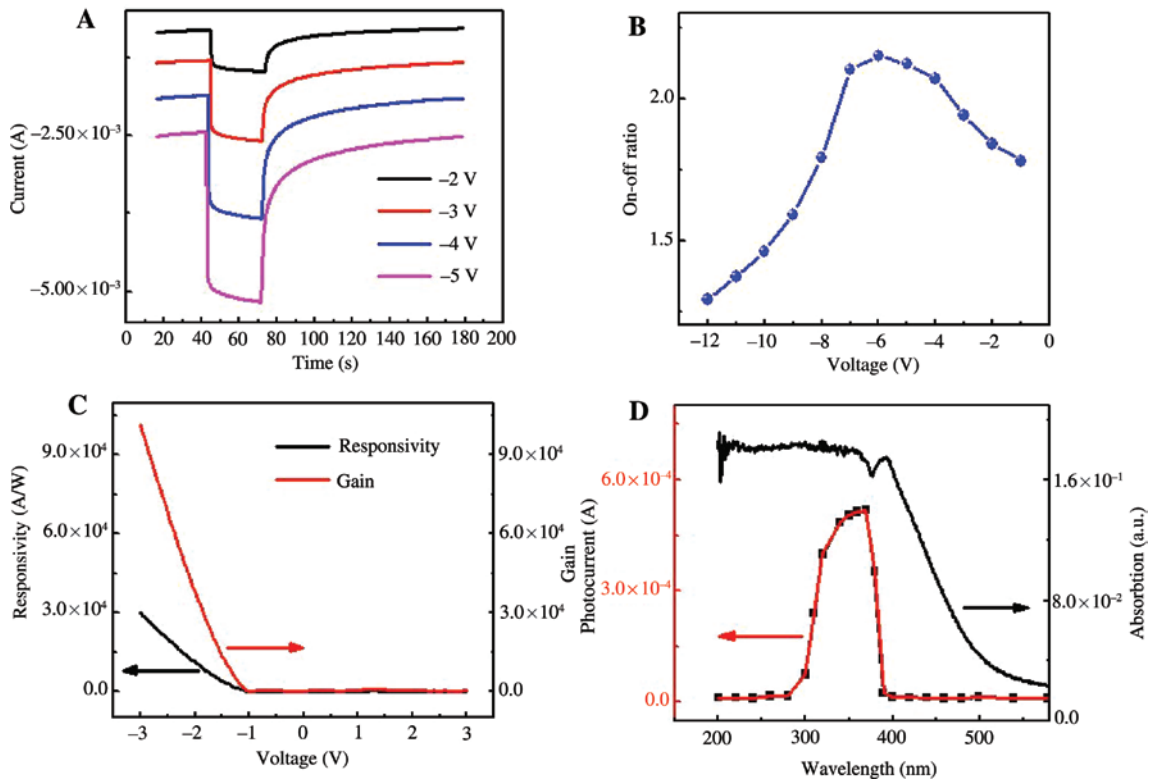

Figure 3: (A) Photoresponse of the UVPD at various bias voltages. (B) The on-off ratios as a function of various bias voltages. (C) Responsivity and gain of the UVPD at various bias voltages. (D) The room temperature absorption (black line) and spectral response of the UVPD (red line) measured at a bias voltage of 5 V.

bias voltage of − 3 V were estimated to be 3×10^4 AW^{-1} and 1×10^5, respectively. The responsivity and gain at different bias voltages are shown in Figure 3C, in which, like the evolution of the on/off ratio, both parameters were observed to increase with decreasing bias voltage. As matter of fact, these two metrics can be further increased when the bias voltage continues to decrease. Figure 3D plots the photocurrent of the UV detector as a function of wavelength. (To make the analysis more reliable, we kept the light power identical for all wavelengths during testing.) It can be seen that the present device exhibits peak sensitivity at 360 nm, corresponding closely to the intrinsic absorption of the ZnO crystal. However, it is virtually blind to irradiation with a wavelength larger than 400 nm or <300 nm. Such spectral response is consistent with the absorption curve (black curve) and is related to the operation mechanism: for light with relatively small energy (e.g. wavelengths larger than 400 nm), the photons have insufficient energy to excite the electrons from the valence band to the conduction band, and therefore, they cannot contribute to the photocurrent. What is more, the slight drop on the shorter wavelength (wavelength <300 nm) is related to the enhanced absorption of high-energy photons at or near the surface region of the ZnO wafer, in this case, the electron-holes generated near the surface region has a relatively shorter lifetime than those in the bulk; thus, they contribute less to the photocurrent.

Next, to determine the resolution limit that could be distinguished from the noise, the specific detectivity (D^*) of the device was calculated by the following equation [30, 31]:

$$D^* = RS^{\frac{1}{2}} \Big/ \left(2qI_d\right)^{\frac{1}{2}} = \Delta I S^{\frac{1}{2}} \Big/ P_{opt}\left(2qI_d\right)^{\frac{1}{2}} \tag{4}$$

where R is the responsivity, S is the effective area of the graphene-ZnO junction, q is the elementary charge, and I_d is the dark current. Using the experimental data mentioned above, the detectivity is calculated to be 4.33×10^{14} Jones. Table 1 summarizes the response rate, responsivity, photoconductive gain, gain-bandwidth product (GBW), and detectivity of the present device and other ZnO-based photodetectors. Compared to other ZnO nanostructure devices, the present graphene-ZnO photodetector has a relatively slow response rate, and the detectivity is comparable to the devices listed below. In addition, the GBW

Table 1: Summary of the performance of the present and other ZnO nanostructure-based devices.

Materials and structures	τ_r	τ_f	R (AW^{-1})	G	GBW	D^* [$cmHz^{1/2}W^{-1}$]	Ref.
Graphene-ZnO wafer	<1 s	<22 s	3×10^4	1×10^5	~10^4	4.33×10^{14}	Our work
ZnO-Ga_2O_3 core-shell	20 μs	42 μs	1.3×10^3	–	–	9.91×10^{14}	[35]
ZnONW array	–	–	4.0	13.8	–	1.27×10^{14}	[33]
Colloidal ZnONPs	<1 s	~1 s	61	203	–	–	[34]
Graphene-ZnONR array	0.7 ms	3.6 ms	113	385	~10^5	–	[21]
ZnONWs	<5 s	<240 s	10^4	–	–	–	[32]

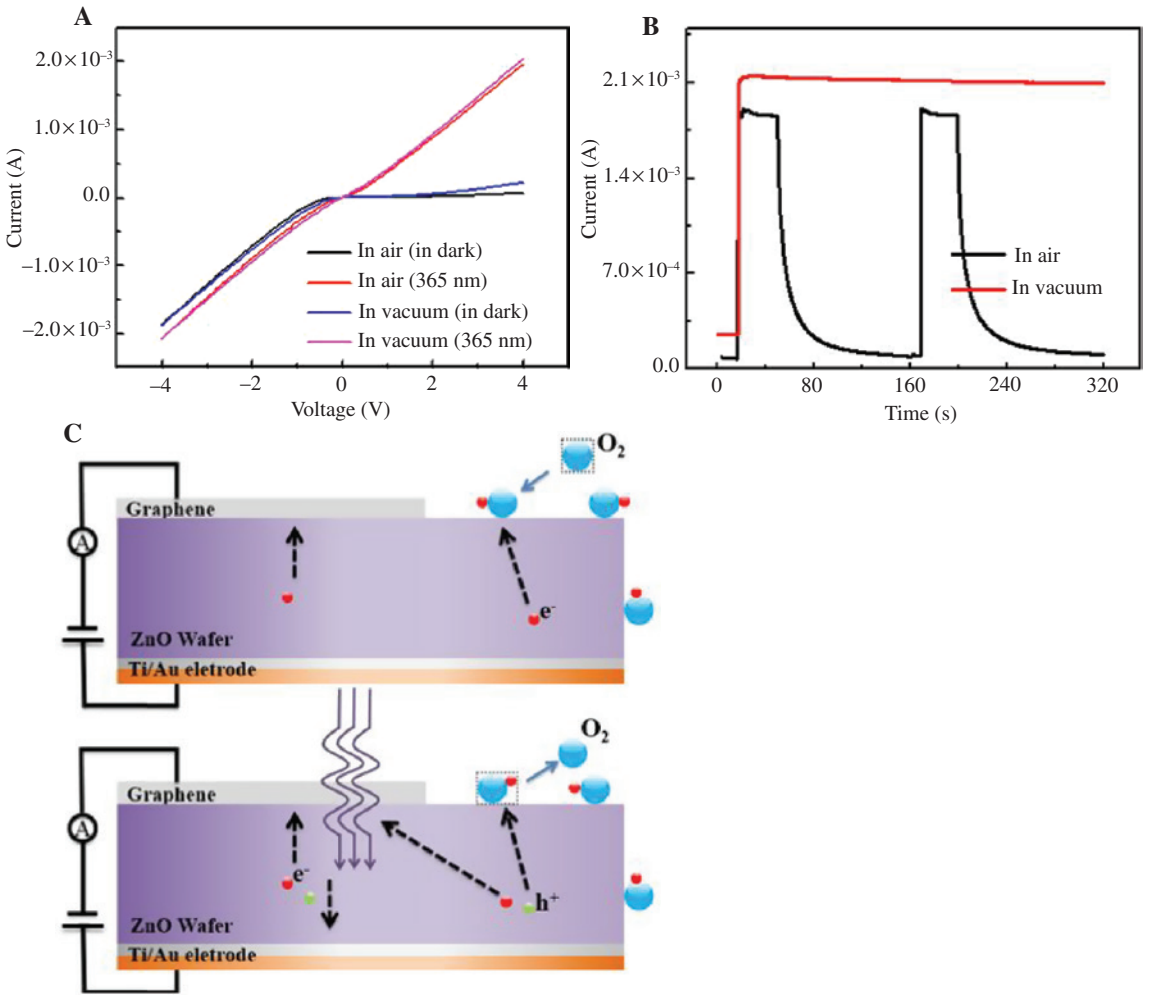

Figure 4: (A) *I-V* characteristics of the UVPD in air and vacuum conditions. (B) Time response of the UVPD measured in air and under vacuum conditions. (C) Schematic illustration of the photosensing mechanism of the graphene-ZnO device under light illumination in a vacuum.

is poorer than the device composed of graphene-ZnONR array. However, it is visible that the graphene-ZnO has an exceptionally high responsivity (3×10^4) and photoconductive gain (10^5), which are not only better than the device solely composed of pure ZnONWs [32], ZnONW array [33], and ZnO nanoparticles (ZnONPs) [34] but also the devices assembled from ZnO-Ga_2O_3 core-shell [35] and graphene-ZnONR array nanocomposite structures [20].

When the graphene-ZnO UVPD was put into a vacuum, it seems that the device can retain its sensitivity to UV light (Figure 4A). The dark current and photocurrent in the dark are 2.4×10^{-4} and 2.1×10^{-3} A, respectively, which are slightly higher than that in air condition (i.e. 7×10^{-5} and 1.8×10^{-3} A). It was also observed that when the UV light was turned off, the response time was considerably elongated. Such a slow response in

vacuum condition is presumably associated with persistent photoconductivity (PPC) effect in which recombination centers play an important role in determining the decay current [36]. As shown in Figure 4C, due to the presence of hole-trap states on the ZnO wafer, oxygen molecules can adsorb onto ZnO surfaces by capturing free electrons from the *n*-type ZnO [$O_2(g) + e^- = O_2^-(ad)$] in air, leading to the formation of a low conductive depletion layer near the surface. The photo-generated holes can migrate to the surface along the potential gradient produced by band bending and recombine with ions to release oxygen [$h^+ + O_2^-(ad) = O_2(g)$]. This recombination process causes the obvious decay photocurrent when illumination light was switched off. In vacuum condition, due to lack of oxygen molecules for the recombination center, the recombination activity is largely restricted. As a result, only holes near the surface can recombine with electrons, leading to a steady-state persistent photocurrent.

It is worth noting that the device performance of such graphene-ZnO UVPD could be optimized when a layer of ultrathin AlO_x was introduced into the device structure. During fabrication, the interfacial passivation layer was actually introduced between the graphene and ZnO wafer, as reported in our previous study [37]. Figure 5A compares both dark current and photocurrent of graphene-ZnO devices with and without passivation layer. Apparently, after interfacial passivation, the dark current decreased a little bit from 2.8×10^{-4} to 2.38×10^{-4} A; however, the photocurrent was considerably increased from 5.85×10^{-4} to 2.89×10^{-3} A (Figure 5B), giving rise to an increase in on/off ratio from 2.09 to 12.1. Understandably, the effective suppression of recombination activities at the ZnO surface, as a consequence of reduced density of surface dangling bonds and defects after passivation of the AlO_x layer is contributory to the improved device performance [38].

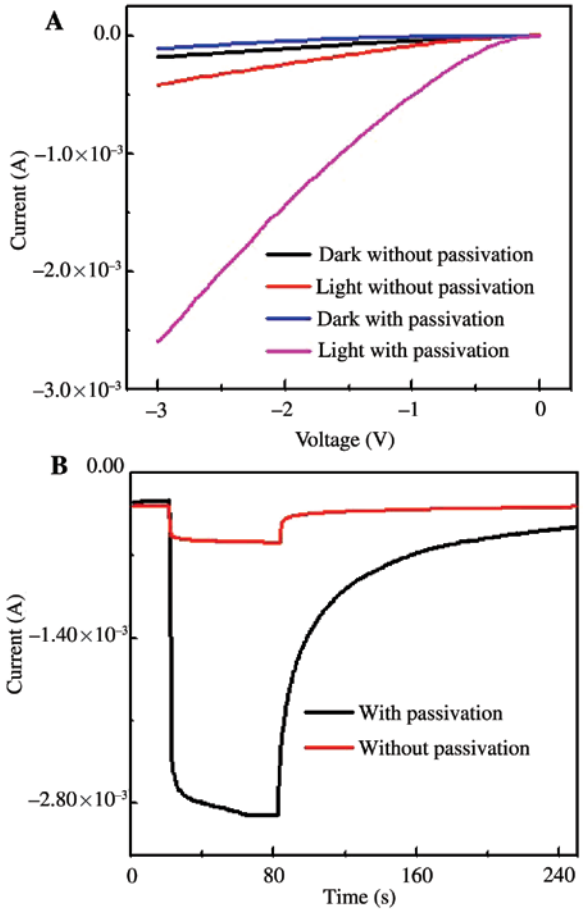

Figure 5: (A) Typical *I-V* characteristic of the graphene-ZnO UVPD with and without AlO_x passivation layer. (B) Photoresponse of both devices with and without light illumination. This study is measured at – 3 V; the light intensity of 365 nm was kept at 0.3 mW/cm² during the test.

3 Conclusion

In conclusion, we demonstrated the fabrication of high-performance UV photodetectors based on graphene-ZnO Schottky junctions. The reponsivity, detectivity, and gain of the device were deduced to be 3×10^4 AW^{-1}, 4.33×10^{14} cm $Hz^{1/2}$ W^{-1}, and 10^5, respectively. These key parameters are much better than other conventional photodetectors based on ZnO. It is expected that this simple, but high-performance, graphene-ZnO device will have potential application for future UV detection.

4 Materials and methods

Materials synthesis: The single-crystalline ZnO substrate, and other reagents were bought from Anhui BEQ equipment Tech. Co., Ltd, Hefei, P. R. China. The specific resistance and the Hall mobility are 4.24×10^2 Ω*cm and -1.117×10^2 cm²/Vs, respectively. The graphene film was synthesized through a CVD method, which was carried out at 1015°C using a mixed gas of CH_4 (1 SCCM) and H_2 (99 SCCM) as reaction source. After growth, the graphene films deposited on Cu foils were spin coated with polymethylmethacrylate (PMMA) solution (5 wt% in chlorobenzene) and then immersed into a Marble's reagent solution ($CuSO_4$: HCl: H_2O = 10 g: 50 ml : 50 ml) to etch away the underlying Cu substrates. To study the structures of the as-synthesized graphene, the PMMA-supported graphene was transferred onto the SiO_2/Si substrate and dried on a hot plate at 100°C for at least 10 min, followed by removal of the PMMA by acetone. The Raman analysis of

the graphene film was performed on a Raman Spectrometer (JY, LabRAM HR800, France).

Device fabrication and characterization: To assemble the graphene film-ZnO UVPDs, the single-crystal ZnO substrate was first cleaned in acetone, alcohol, and deionized water, respectively, to remove possible contaminants. The substrate that was partially pasted with Sellotape was then soaked in deionized water and then slowly lifted to mount the graphene film on the single-crystal ZnO substrate. Finally, a drop of silver paste was adhered to the graphene where PMMA film was removed by acetone. The electrical property of the UVPDs was analyzed using a semiconductor characterization system (Keithley 4200-SCS, USA). To study the optoelectronic properties, incident lights from both xenon lamp (150 μW) and a monochromator (SP2150, Princeton Co., USA) were vertically focused and guided onto the device. The low-temperature *I-V* measurements in the temperature range of 80 to 300 K were carried out on the semiconductor characterization system (4200-SCS, Keithley Co.) equipped with an automatic cooling system (CCS-350 Slow temperature cycle refrigeration system, East Changqing Co., China).

Acknowledgments: This work was supported by the Natural Science Foundation of China (NSFC, Nos., 61575059, 61675062) and the Fundamental Research Funds for the Central Universities (2012HGCX0003, 2013HGCH0012, 2014HGCH0005).

References

[1] Jie JS, Zhang WJ, Bello I, Lee CS, Lee ST. One-dimensional II-VI nanostructures: synthesis, properties and optoelectronic applications. Nano Today 2010;5:313–36.
[2] Liu R,You XC, Fu XW, et al. Gate modulation of graphene-ZnO nanowire Schottky diode. Sci Rep 2015;5:10125.
[3] Lao CS, Liu J, Gao PX, et al. ZnO nanobelt/nanowire Schottky diodes formed by dielectrophoresis alignment across Au electrodes. Nano Lett 2006;6:263.
[4] Lee JM, Pyun YB, Yi J, Choung JW, Park WI. ZnO nanorod-graphene hybrid architectures for multifunctional conductors. J Phys Chem C 2009;113:19134–8.
[5] Gupta MK, Sinha N, Kumar B. P-type k-doped ZnO nanorods for optoelectronics applications. J Appl Phys 2011;109:083532.
[6] Djurišić AB, Ng AMC, Chen XY. ZnO nanostructures for optoelectronics: material properties and devices applications. Prog Quant Electron 2010;34:191–259.
[7] Wan Q, Li QH, Chen YJ, et al. Fabrication and ethanol sensing characteristics of ZnO nanowire gas sensors. Appl Phys Lett 2004;84:3654–6.
[8] Al-Hilli SM, Willander M, Öst A, Strålfors P. ZnO nanorod as an intracellular sensor for pH measurements. J Appl Phys 2007;102:084304.
[9] Fan ZY, Wang DW, Chang PC, Tseng WY, Lu JG. ZnO nanowire field-effect transistor and oxygen sensing property. Appl Phys Lett 2004;85:5923–5.
[10] Özgür Ü, Alivov YI, Liu C, et al. A comprehensive review of ZnO materials and devices. J Appl Phys 2005;98:041301.
[11] Zhang QF, Dandeneau CS, Zhou XY, Cao GZ. ZnO nanostructures for dye-sensitized solar cells. Adv Mater 2009;21:4087–108.
[12] Weng WY, Chang SJ, Hsu CL, Hsueh TJ. A ZnO-nanowire phototransistor prepared on glass substrate. ACS Appl Mater Interfaces 2011;3:162–6.
[13] Bao JM, Zimmler MA, Capasso F. Broadband ZnO single-nanowire light-emitting diode. Nano Lett 2006;6:1719–22.
[14] Lee YS, Jung YI, Noh BY, Park IK. Emission pattern control of GaN-based light-emitting diodes with ZnO nanostructures. Appl Phys Express 2011;4:112101.
[15] Huang MH, Mao S, Feick H, et al. Room-temperature ultraviolet nanowire nanolasers. Science 2001;292:1897.
[16] Johnson JC, Yan HQ, Yang PD, Saykally RJ. Optica cavity effects in ZnO nanowire lasers and waveguides. J Phys Chem B 2003;107:8816–28.
[17] Law JBK, Thong JTL. Simple fabrication of a ZnO nanowire photodetector with a fast photoresponse time. Appl Phys Lett 2006;88;133114.
[18] Hatch SM, Briscoe J, Dunn S. A self-powered ZnO-nanorod/CuSCN UV photodetector exhibiting rapid response. Adv Mater 2013;25:867–71.
[19] Liu KW, Sakurai M, Aono M. ZnO-based ultraviolet photodetectors. Sensors 2010;10:8604–34.
[20] Soci C, Zhang A, Xiang B, et al. ZnO nanowire UV photodetectors with high internal gain. Nano Lett 2007;7:1003–9.
[21] Nie B, Hu JG, Luo LB, et al. Monolayer graphene film on ZnO nanorod array for high-performance Schottky junction ultraviolet photodetectors. Small 2013;9:2872–9.
[22] Xie C, Jie JS, Nie B, et al. Schottky solar cells based on graphene nanoribbon/multiple silicon nanowires junctions. Appl Phys Lett 2012;100:193103.
[23] Jin WF, Ye Y, Gan L, et al. Self-powered high performance photodetectors based on CdSe naobelt/graphene Schottky junctions. J Mater Chem 2012;22:2863–7.
[24] Chen HY, Liu KW, Chen X, et al. Realization of a self-powered ZnO MSM UV photodetector with high responsivity using an asymmetric pair of Au electrodes. J Mater Chem C 2014;2:9689–94.
[25] Miao XC, Tongay S, Petterson MK, et al. High efficiency graphene solar cells by chemical doping. Nano Lett 2012;12:2745–50.
[26] Wang MZ, Liang FX, Nie B, et al. TiO_2 nanotube array/monolayer graphene film Schottky junction ultraviolet light photodetectors. Part Syst Charact 2013;30:630–6.
[27] Jie JS, Zhang WJ, Jiang Y, Meng XM, Li YQ, Lee ST. Photoconductive characteristics of single-crystal CdS nanoribbons. Nano Lett 2006;6:1887–92.
[28] Chen Q, Ding HY, Wu YK, et al. Passivation of surface states in the ZnO nanowire with thermally evaporated copper phthalocyanice for hybrid photodetectors. Nanoscale 2013;5:4162–5.
[29] Yang C, Barrelet CJ, Capasso F, Lieber CM. Single p-type/intrinsic/n-type silicon nanowires as nanoscale avalanche photodetectors. Nano Lett 2006;6:2929–34.
[30] Gong X, Tong MH, Xia YJ, et al. High-detectivity polymer photodetectors with spectral response from 300 nm to 1450 nm. Science 2009;325:1665–7.

[31] Manga KK, Wang JZ, Lin M, et al. High-performance broadband photodetectors using solution-processable Pb-TiO_2-graphene hybrids. Adv Mater 2012;24:1697–702.
[32] Zhang H, Babichev AV, Jacopin G, et al. Characterization and modeling of a ZnO nanowire ultraviolet photodetector with graphene transparent contact. J Appl Phys 2013;114:234505.s
[33] Leung YH, He ZB, Luo LB, Tsang CHA, Wong NB. ZnO nanowire array p-n homojunction and its application as a visible-blind ultraviolet photodetector. Appl Phys Lett 2010;96:053102.
[34] Jin YZ, Wang JP, Sun BQ, Blakesley JC, Greenham NC. Solution-processed ultraviolet photodetectors based on colloidal ZnO nanoparticles. Nano Lett 2008;8:1649–53.
[35] Zhao B, Wang F, Chen HY, et al. Solar-blind avalanche photodetector based on single ZnO-Ga_2O_3 core-shell microwire. Nano Lett 2015;15:3988–93.
[36] Huang K, Zhang Q. Giant persistent photoconductivity of the WO_3 nanowires in vacuum condition. Nanoscale Res Lett 2011;6:52.
[37] Luo LB, Hu H, Wang XH, et al. A graphene/GaAs near-infrared photodetector enabled by interfacial passivation with fast response and high sensitivity. J Mater Chem C 2015;3:4723–8.
[38] Tajik N, Peng Z, Kuyanov P, LaPierre RR. Sulfur passivation and contact methods for GaAs nanowire solar cells. Nanotechnology 2011;22:225402.